arXiv:1409.6085v2 [cond-mat.mtrl-sci] 10 Nov 2014

Stable and Efficient Linear Scaling First-Principles Molecular Dynamics for 10,000+ atoms

Michiaki Arita,[†,‡] David R. Bowler,[¶,§,‖] and Tsuyoshi Miyazaki[*,‡,†]

Faculty of Science and Technology, Tokyo University of Science, 2641 Yamasaki, Noda, Chiba 278-8510, Japan, Computational Materials Science Unit (CMSU), National Institute for Materials Science (NIMS), 1-1 Namiki, Tsukuba, Ibaraki 305-0044, Japan, Department of Physics and Astronomy, University College London (UCL), Gower Street, London WC1E 6BT, UK, London Centre for Nanotechnology(LCN), University College London (UCL), 17-19 Gordon Street, London WC1H 0AH, UK, and International Center for Materials Nanoarchitectonics (MANA), National Institute for Materials Science (NIMS), 1-1 Namiki, Tsukuba, Ibaraki 305-0044, Japan

E-mail: MIYAZAKI.Tsuyoshi@nims.go.jp

Abstract

The recent progress of linear-scaling or O(N) methods in the density functional theory (DFT) is remarkable. Given this, we might expect that first-principles molecular dynamics (FPMD) simulations based on DFT could treat more realistic and complex systems using the O(N) technique. However, very few examples of O(N) FPMD simulations exist so far and the information for the accuracy or reliability of the simulations is very limited. In this paper, we

[*]To whom correspondence should be addressed
[†]Tokyo University of Science
[‡]CMSU, NIMS
[¶]Physics and Astronomy, UCL
[§]LCN, UCL
[‖]MANA, NIMS

show that efficient and robust O(N) FPMD simulations are now possible by the combination of the extended Lagrangian Born-Oppenheimer molecular dynamics method, which was recently proposed by Niklasson *et al* (*Phys. Rev. Lett.* 100, 123004 (2008)), and the density matrix method as an O(N) technique. Using our linear-scaling DFT code CONQUEST, we investigate the reliable calculation conditions for the accurate O(N) FPMD and demonstrate that we are now able to do practical, reliable self-consistent FPMD simulation of a very large system containing 32,768 atoms.

1 Introduction

First-principles molecular dynamics (FPMD) based on density functional theory (DFT) is a well-established and highly-successful tool for studying reactions or processes of materials at the atomic scale. Due to the increase of the computer power, the variety and complexity of the materials and phenomena investigated by FPMD simulations have been growing. However, the size of the systems modelled with FPMD simulations have remained limited to systems of a few hundred atoms in most cases, because the computational cost of standard DFT methods grow rapidly, proportional to the cube of the number of atoms N in the system. There are many demands to enlarge the system size in diverse fields, including computational physics, chemistry, materials science, biology and so on. Examples of these problems include chemical reactions at liquid/solid interfaces, various processes in complex biological systems, or the growth mechanism of the nano-structured materials at atomic scale; in all these cases, we have to treat systems containing many thousands or tens of thousands of atoms. In this respect, recent advances in developing linear-scaling or O(N) methods are encouraging.[1] There have been several demonstrations that efficient and reliable linear-scaling DFT calculations are now available to calculate the electronic structure, total energy and atomic forces of very large systems, including up to millions of atoms.[2,3]

Although it is now possible to calculate the total energy and atomic forces of very large systems using O(N) DFT methods,[4–7] this does not guarantee that stable, efficient and accurate FPMD simulations are possible in practice.[8] With conventional DFT methods, there are two widely-used

methods to achieve efficient FPMD simulations. The first method is known as Car-Parrinello MD (CPMD),[9] where the propagation of electronic structure and the atomic positions are treated simultaneously by introducing a fictitious mass for the electronic degree of freedom. This method is efficient, but the accuracy of the CPMD simulations can depend on the choice of the fictitious mass. By contrast, Born-Oppenheimer MD (BOMD) deals with the electronic and nuclear problems separately. In this method, the electronic structure in the ground state is calculated at each set of atomic positions, usually by the optimization of the Kohn-Sham orbitals using an iterative method.[10] The BOMD method thus needs more CPU time than CPMD for each MD step, but the method is robust and stable, and allows us to adopt a longer time step. As a result, the CPU time needed for a whole MD simulation is tractable because the number of force calculations is smaller (the cost of calculating atomic forces is usually much higher than the update of the Kohn-Sham orbitals). The main problem facing this method, however, is that both the stability and the reliability of the MD depend on the accuracy of the calculated forces. If the optimization of the Kohn-Sham orbitals or the convergence of SCF is not sufficiently accurate, the method suffers from a systematic energy drift in micro-canonical MD simulations, due to the violation of time-reversal symmetry. This can also result in poor reliability for canonical MD simulations. Recently this problem has been solved using the extended Lagrangian Born-Oppenheimer MD (XL-BOMD) proposed by Niklasson et al.,[11–13] whose Lagrangian includes auxiliary electronic degrees of freedom as dynamical variables to recover time-reversal symmetry in BOMD simulations. They have shown that BOMD simulations with long-term conservation of total energy are possible.

It is reasonable to expect that this recent progress with the XL-BOMD method could be used with O(N) DFT techniques. However, since linear-scaling methods rely on the locality of the electronic structure and need to introduce approximations to utilize this locality, the accuracy of O(N) method may change during the MD simulations, and it is not clear how accurate or stable MD can be with O(N) DFT methods. Although there have been already a few reports showing the examples of O(N) FPMD[14–17] or O(N) self-consistent tight-binding[18] simulations, they use different linear scaling techniques and the information about the accuracy, stability or efficiency

of the simulations is rather limited. In this paper, we report the stability and accuracy of the XL-BOMD simulations with a density matrix minimization (DMM) technique,[19,20] which is one of the most common O(N) DFT methods. The accuracy of the forces calculated by the DMM method is high because the method satisfies the variational principle.[5] To our knowledge, the combination of DMM and XL-BOMD methods has not been investigated so far. Since the original XL-BOMD methods assume the orthogonality of the basis functions, the formulation of the method for non-orthogonal basis functions is also presented. We show that the XL-BOMD method can be introduced to our linear-scaling DFT code CONQUEST,[21–23] and report that robust, accurate and efficient FPMD is possible with the DMM method. The reliable calculation conditions for the accurate O(N) FPMD are also investigated. In the end, we demonstrate that it is now possible to do actual FPMD simulations of a 32,768-atom system.

The rest of the paper is organized as follows. In the next section, we show the methods and algorithms which are used or introduced in this work. In Sec. 3, we report the results of the test calculations, investigation of the reliable calculation conditions, and some examples of the FPMD simulations, including that of 32,768-atom system. Finally, concluding remarks are given in Sec. 4.

2 Methods and Algorithms

The implementation of molecular dynamics and all calculations were performed with CONQUEST, which is a linear scaling, pseudopotential DFT code.[21–23] In order to achieve linear-scaling both in computational time and memory consumption, the code works with the density matrix ρ rather than the wavefunctions, because of its spatial locality:

$$\rho\left(r,r'\right) \to 0 \text{ as } |r-r'| \to \infty. \tag{1}$$

CONQUEST assumes that the density matrix can be described in a separable form:

$$\rho(r,r') = \sum_{i\alpha,j\beta} \phi_{i\alpha}(r) K_{i\alpha,j\beta} \phi_{j\beta}(r'), \tag{2}$$

where $\phi_{i\alpha}$ is a non-orthogonal localised orbital called a *support function*, which is only non-zero within a sphere centred at atom i, and α denotes the support functions of a given atom.

Support functions are represented in terms of localised basis functions; in CONQUEST we can use systematically improvable basis functions (B-splines[24]) or pseudoatomic-orbitals (PAOs).[4,25] $K_{i\alpha,j\beta}$ is the density matrix represented in terms of the support functions. We find the electronic ground state by minimising the total energy with respect to the density matrix, while imposing the correct electron number and weak idempotency. The complete minimisation combines two algorithms:[26] McWeeny's iterative purification;[27,28] and the auxiliary density matrix (ADM) method proposed by Li, Nunes and Vanderbilt.[19] An initial density matrix is generated starting from the Hamiltonian (scaled to have the right trace and eigenvalue spectrum), using the extension of McWeeny's approach for the canonical case.[28]

In the ADM method, weak idempotenty is imposed by expressing the density matrix K in terms of an auxiliary density matrix L, and the overlap S between support functions, $S_{i\alpha,j\beta} =< \phi_{i\alpha}|\phi_{j\beta} >$, as

$$K = 3LSL - 2LSLSL \tag{3}$$

The spatial truncation on the density matrix is actually imposed on the matrix L, such that $L_{i\alpha,j\beta} = 0$ once $|R_i - R_j| \geq R_L$; this is referred as *L-range* in the rest of this report.

The McWeeny's procedure is applied until the energy rises (a sign of reaching truncation error[28]). The L matrix is then passed into the ADM, which is a variational approach, using a modified Pulay/Broyden algorithm. This part of the minimisation is referred to as DMM (density matrix minimisation).

In this paper, we represent each support function $\phi_{i,\alpha}(r)$ in terms of one PAO (the approach given here is easily extended to the case where we also minimise the energy with respect to the PAOs, which will be presented in a future publication). In running BOMD simulations with the DMM method, we have two ways to optimize the electronic structure. One is to initialise the density matrix using McWeeny's procedure at every atom movement. The initial charge density is made from the superposition of the atomic charge density. Since the Hamiltonian and overlap matrices are recalculated after the movement of atoms, the initial matrix L and subsequent optimised L matrix will maintain time-reversal symmetry; we hence expect that BOMD simulations should conserve energy and be stable. The other method is to utilize the auxiliary density matrix found from the previous MD step to start the present DMM. In this case, the initial charge density is made from the initial density matrix L prepared for the present DMM, and is updated with the L matrix simultaneously during the DMM. This method will be more efficient, but will break time reversal symmetry, potentially leading to unphysical energy drift.

To maintain time-reversal symmetry while keeping the efficiency of density matrix re-use, we will use the extended Lagrangian scheme proposed by Niklasson et al.[12] We introduce an auxiliary degree of freedom to the Born-Oppenheimer Lagrangian $\mathscr{L}^{\mathrm{XBO}}$, X. This is associated with LS, rather than L to maintain the correct non-orthogonal metric.[29]

$$\mathscr{L}^{\mathrm{XBO}}\left(X,\dot{X},R,\dot{R}\right)=\mathscr{L}^{\mathrm{BO}}\left(R,\dot{R}\right)+\frac{\mu}{2}\mathrm{Tr}\left[\dot{X}^2\right]-\frac{\mu\omega^2}{2}\mathrm{Tr}\left[(LS-X)^2\right] \tag{4}$$

X is a sparse matrix with the range of the matrix LS, μ the fictitious electronic mass, and ω is the curvature of the electronic harmonic potential. As in the original XL-BOMD method, if we take the limit $\mu \to 0$, $\mathscr{L}^{\mathrm{XBO}}$ becomes $\mathscr{L}^{\mathrm{BO}}$ and we have equations of motion for nuclear positions and X. If we apply the time-reversible Verlet scheme to calculate X using the equation of motion, we have

$$X(t+\delta t)=2X(t)-X(t-\delta t)+\delta t^2\omega^2(L(t)S(t)-X(t)) \tag{5}$$

which shows that $X(t)$ is time reversible and evolves in a harmonic potential centered around the ground-state $L(t)S(t)$. This also implies that a good initial guess for the L-matrix, which will obey time reversal symmetry, can be calculated by multiplying X and S^{-1} (in CONQUEST, the sparse approximate inverse S is computed using Hotelling's method[30]).

Even though the time-reversibility is maintained during propagation, the X-matrix tends to move away from the harmonic centre over time. As a result, the number of iterations to reach the ground state at each MD step gradually increases in the course of a simulation. To remove accumulated numerical errors, we add a dissipative force to the propagation of X following Ref.,[31]

$$X(t+\delta t) = 2X(t) - X(t-\delta t) + \kappa(L(t)S(t) - X(t)) + \alpha \sum_{m=0}^{M} c_m X(t - m\delta t). \tag{6}$$

Here, the parameters κ, α and c_m are determined so that the dissipation term does not significantly break the time-reversal symmetry; we use the values in Ref.[31] The amount of dissipation is controlled with a single parameter M, which determines the order of the polynomial, and we use $M = 5$ in this paper. With the dissipation term, we can keep the kinetic energy of $\dot{X}$ small and thus the $X(t)$ is kept close to the present ground-state $L(t)S(t)$. As a result, we expect that the number of DMM steps would be reduced. The effect of the dissipation term in the practical calculations is reported and discussed in Sec. 3.1.

3 Results

We will present our tests of the implementation of O(N) DFT in different stages: first, considering approaches that permit energy conservation and their efficiencies; second, the effect of density matrix range and minimisation tolerance; and finally presenting practical calculations.

3.1 Effective schemes for linear-scaling BOMD

First, we explore methods to achieve energy conservation with O(N) DFT and BOMD. We monitor the Born-Oppenheimer total energy E_{BO}, which is defined as a sum of the ionic kinetic energy T and the DFT total energy V_{BO}. In the micro-canonical ensemble, E_{BO} should be constant and so is a good indicator to judge whether a simulation is accurately carried out. In what follows, R_L is set to 16 bohr (the effect of changing this is explored below in Sec. 3.2). A single-ζ (SZ) PAO is used to represent support functions,[32] and the local density approximation (LDA) is adopted to the exchange-correlation functional with the parametrization by Perdew and Zunger.[33] MD simulations are conducted via the velocity-Verlet integrator[34] with a time step being 0.5 femtoseconds (fs) in a micro-canonical ensemble; the initial velocities are given randomly so that the Maxwell-Boltzmann distribution holds with 300 K. The same conditions are set in other simulations in this report unless otherwise specified.

For a first run, we perform BOMD on a 64-atom crystalline silicon with density-matrix initialisation by McWeeny step, so that the density matrix is initialised from the Hamiltonian at each MD step. The density matrix is updated until the residual in the DMM step, $\frac{1}{N}\mathrm{Tr}(\sigma S^{-1}\sigma S^{-1})$ with $\sigma = \delta E'/\delta L$, becomes smaller than a given tolerance ε_L. Here, E' is defined as $V_{\mathrm{BO}} - \mu N_{\mathrm{el}}$, the number of electrons is N_{el} and the Lagrange multiplier μ is used to keep the electron number fixed. The profile of the Born-Oppenheimer energy E_{BO} is shown by a solid line in Fig. 1, and it is clear that the total energy is conserved even for a low DMM tolerance, $\varepsilon_L = 1.6 \times 10^{-5}$. This simulation is, however, time-consuming since the electronic structure is calculated from scratch at every atom movement.

We now consider the re-use of the optimised L-matrix from the previous MD step. When the optimised L-matrix from the previous step is used to initialise the density matrix, the CPU time is significantly reduced. However, as well as this improved efficiency, we observe a significant and undesired energy drift, as shown in Fig. 1 with symbols. Here, we consider various values for the tolerance applied to the density matrix minimisation, ε_L. The energy drift can be reduced by using a tighter ε_L, but tighter tolerance rapidly increases the number of DMM iterations and the

computational cost.

In order to solve the problem of both accuracy and efficiency, we carry out XL-BOMD with a DMM tolerance, $\varepsilon_L = 1.6 \times 10^{-5}$. Its E_{BO} profile (crosses in Fig. 2) agrees extremely well with that of BOMD with density-matrix initialisation by means of McWeeny step (solid line in Fig. 2), implying that XL-BOMD yields a well conserved energy with lower computational requirements. However, there is a problem in the efficiency with the method, as explained in Sec. 2. After a long simulation time, the number of DMM iterations required to find the ground state density matrix grows. This growing cost can be suppressed by applying a dissipative force, and the resulting E_{BO} profile, circles in Fig. 2, is still very close to the profile without dissipation. A comparison of the required number of DMM iterations at each step for these different approaches is shown in Table. 1. The reduction of computational cost by using XL-BOMD with dissipation is significant. Besides the smaller number of DMM iterations, the method does not require McWeeny steps which typically include a few tens of matrix multiplications for purification (as in Eq. 3).

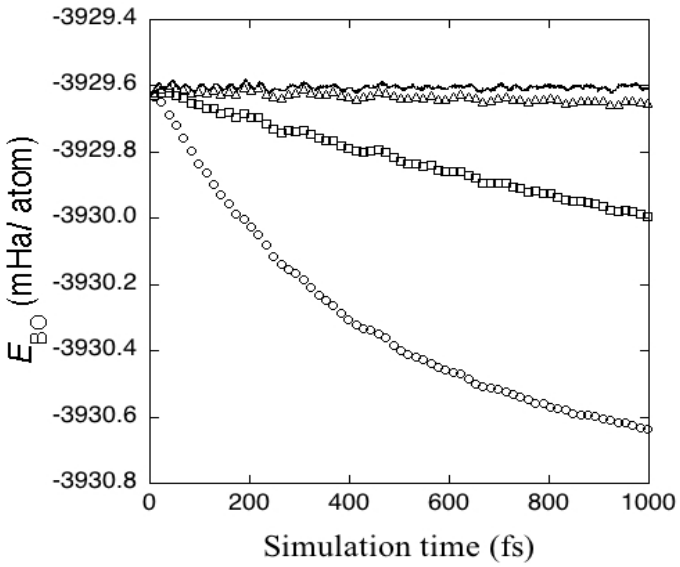

Figure 1: Born-Oppenheimer total energy profiles obtained with McWeeny initialisation at every step (solid line) and by reusing the L-matrix from the previous step for different tolerances (symbols). Symbols stand for tolerance ε_L taking values 1.6×10^{-5} (circle), 1.6×10^{-7} (square) and 1.6×10^{-9} (triangle).

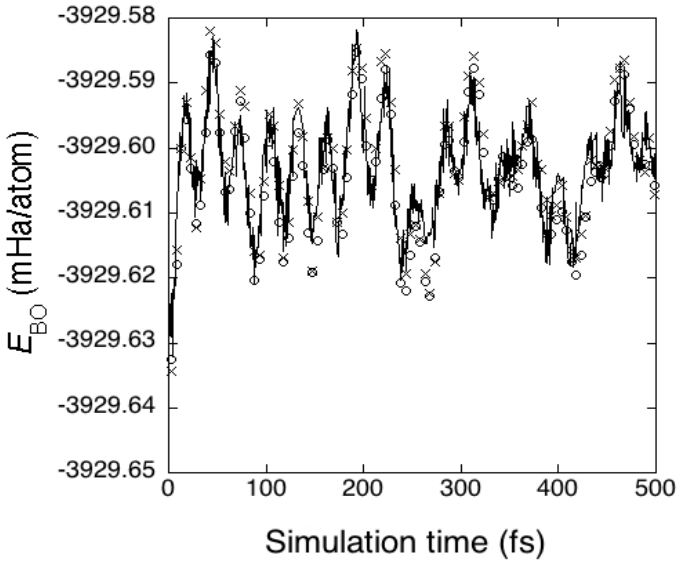

Figure 2: Born-Oppenheimer total energy profiles with tolerance ε_L 1.6×10^{-5}, and different initialisations: McWeeny initialisation at each MD step (solid line); XL-BOMD with dissipative force (circles); and XL-BOMD without dissipative force (crosses).

Table 1: DMM iterations required for each MD step; BOMD with density-matrix initialisation by McWeeny step, and XL-BOMD in the presence (Y) and absence (N) of a dissipative force. Averages taken over 1,000 steps.

type of run	dissipation	average	max	min
BOMD	N	10	12	8
XL-BOMD	N	6.7	8	2
XL-BOMD	Y	3.9	4	2

3.2 Effects of density matrix tolerance and range on XL-BOMD

In the last section, we showed that XL-BOMD simulation with DMM method was robust and efficient using one typical set of calculation conditions. We now investigate how MD results are affected by the parameters which control the accuracy and efficiency of linear-scaling DFT calculations with DMM. There are two key parameters: the range applied to the auxiliary density matrix (L-range or R_L); and the tolerance applied to the minimisation, ε_L. In both tests, XL-BOMD is performed on a 64-atom crystalline silicon with a dissipative force.

3.2.1 R_L-dependence

The key approximation made in linear scaling is to localize the density matrix, and it is vital to examine how the conservation of energy, E_{BO}, is affected by the range, the parameter R_L. We have tested three values of R_L: 13, 16 and 20 bohr, each with a strict DMM tolerance, $\varepsilon_L = 1.6 \times 10^{-7}$. Simulations are performed for 2ps (or 4,000 steps).

The time-averaged BO total energies are very different for the three ranges (-106.830 eV/atom, -106.930 eV/atom and -106.987 eV/atom) simply because the potential energy is lower for longer ranges. We plot the instantaneous energy fluctuations for the three ranges in Fig. 3; the time-averaged absolute fluctuations, $\langle|\Delta E_{BO}|\rangle$, are 0.24 meV/atom, 0.15 meV/atom and 0.075 meV/atom. These fluctuations become smaller as the range increases, and no energy drift is seen for any of the ranges.

During MD, atoms will move in and out of the density matrix range, and we might expect to see energy drift and deviations at small ranges, compared to long ranges. The lack of drift is extremely encouraging, showing that the XL-BOMD approach is well-suited both to orthogonal and non-orthogonal basis sets, and linear scaling approaches. It is also encouraging that, for relatively modest ranges, good accuracy is seen. We plot the kinetic energy of the ions in Fig. 4, which shows that, while there is a deviation for 13 bohr range after 2-300 femtoseconds, the 16 bohr range profile is extremely close to the 20 bohr range profile, and therefore this range can be used with confidence over at least 1ps.[35]

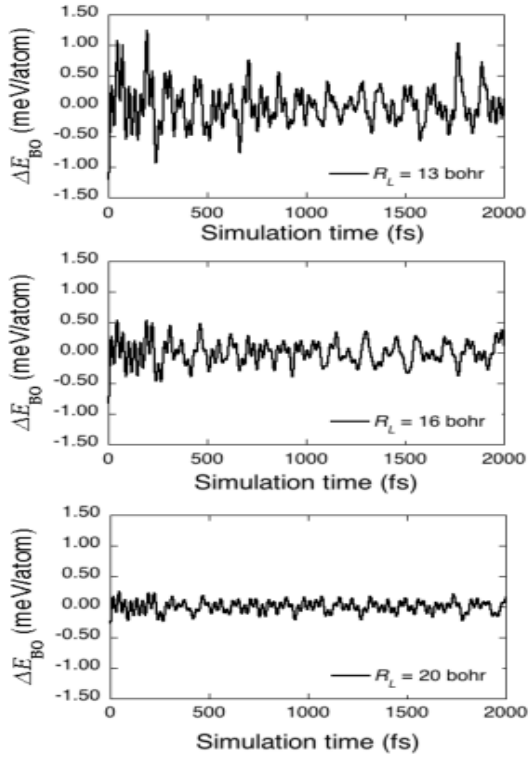

Figure 3: The instantaneous energy fluctuations calculated by three R_L values; 13 bohr (top), 16 bohr (middle) and 20 bohr (bottom).

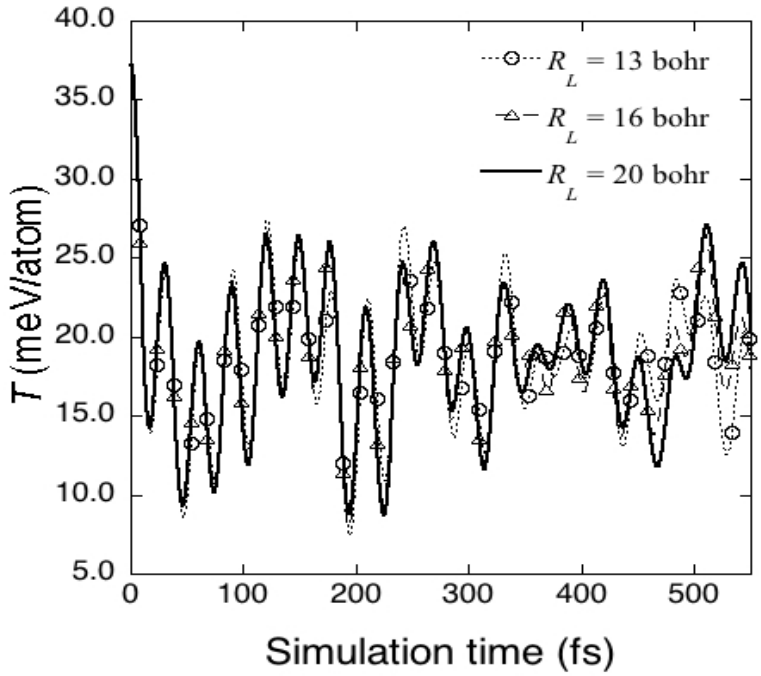

Figure 4: The ionic kinetic energy profiles by three R_L values; 13 bohr, 16 bohr and 20 bohr.

3.2.2 ε_L-dependence

The other main parameter which must be tested for its effect on the accuracy and stability of linear-scaling MD is the DMM tolerance ε_L. From the results of the last section, we fix the L-range to 16 bohr and apply a wide range of ε_L from 10^{-4} to 10^{-7}; we assume that the results with $\varepsilon_L = 10^{-7}$ can be regarded as reference values. We plot the BO total energy over a set of 1ps simulations in Fig. 5. First we note that E_{BO} with $\varepsilon_L = 10^{-4}$ (circles) is not fully converged, and is higher in energy by about 2 meV/atom than the converged one. However, as we see in Fig. 6, the kinetic energy profile shows almost perfect agreement with the reference profile of $\varepsilon_L = 10^{-7}$, indicating that forces and hence the ionic kinetic energy converge faster than the total energy. Note that we can achieve good convergence for both E_{BO} and T with $\varepsilon_L = 10^{-5}$. In addition, the E_{BO} profiles are close to each other for all tolerances except for a constant shift of the energy. Given the fast convergence in ionic kinetic energy, and the similarities in E_{BO} profiles, the calculated trajectories will be very close. Hence, the DMM tolerance of 10^{-4} will give an accurate simulation.

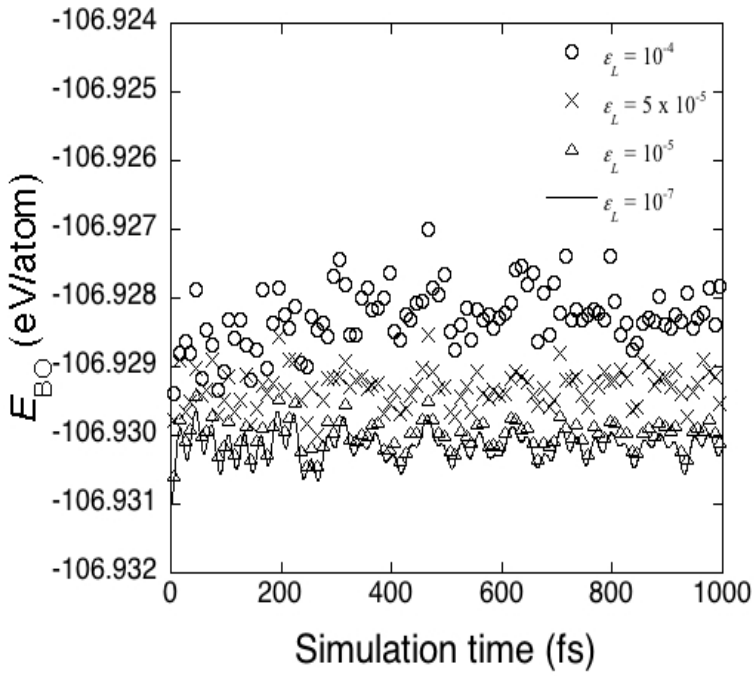

Figure 5: The Born-Oppenheimer total energy profiles calculated for different ε_L values: circles, squares and triangles denote the profiles given by $\varepsilon_L = 10^{-4}$,5×10^{-5} and 10^{-5}, respectively. The solid line shows the profile calculated with $\varepsilon_L = 10^{-7}$.

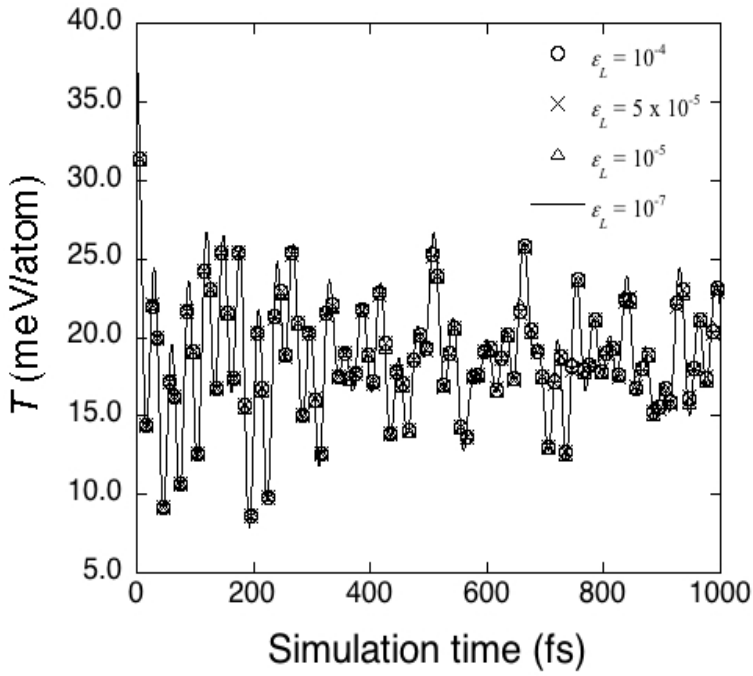

Figure 6: The ionic kinetic energy profiles calculated for different ε_L values: circles, crosses and triangles denote the profiles given by $\varepsilon_L = 10^{-4}$,5×10^{-5} and 10^{-5}, respectively. A solid line shows the profile calculated with $\varepsilon_L = 10^{-7}$.

3.3 Practical $\mathscr{O}(N)$-MD simulations

Having investigated the effects of the parameters on simulations, we now present applications of the CONQUEST code to practical MD simulations using a double-ζ + polarisation (DZP) PAO basis, which is commonly used as a converged basis set. Three different systems are presented: 8-atom crystalline silicon; 32 water molecules; and a 32,768-atom crystalline silicon cell to demonstrate application to a large system. For all systems, L range is set to 16 bohr. The initial temperature is 300K and the time step of the simulation is 0.5 femtosecond, unless stated otherwise.

3.3.1 Eight atom bulk silicon

Our first example is a small sample of crystalline silicon. We show the BO energy, E_{BO}, calculated with ε_L set to 1.3×10^{-4} in Figure 7. This plot demonstrates excellent energy conservation, though there are large fluctuations for the first few femtoseconds. This initial large amplitude is probably

caused by the system not being in an equilibrium state at the start of the simulation, and is not a significant problem. In the inset of Fig. 7, we also show the result of a simulation where we set $S = 1$ in Eq. 4 or Eq. 5 (by supposing that L is expressed using orthogonal basis sets). By comparing the result (dotted line) with the correct one (solid line), we see that the former energy exhibits significant drift, while the latter one is well behaved. This indicates the importance of the metric used for non-orthogonal basis functions.

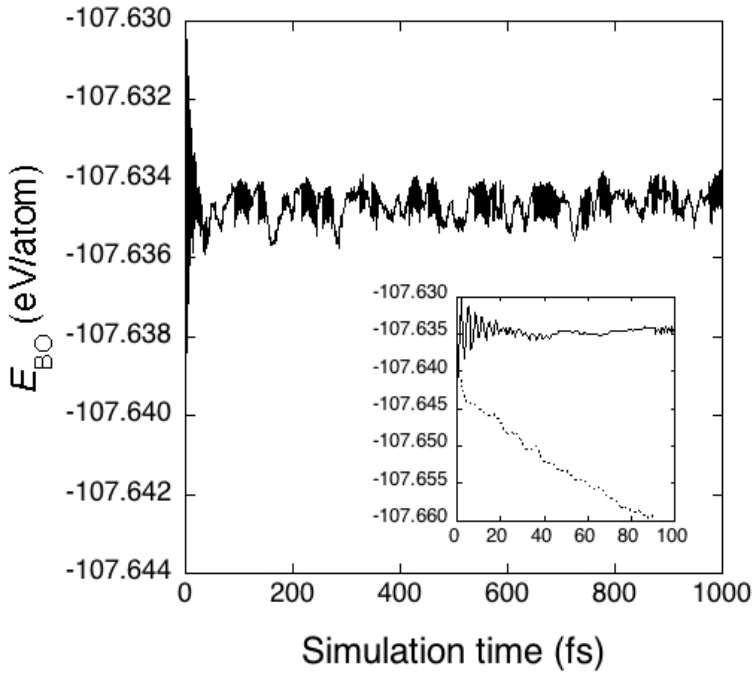

Figure 7: Main: Born-Oppenheimer total energy profile of crystalline Si with a DZP basis set. Inset: comparison of two approaches to XL-BOMD, solid and dotted lines indicating the corrected and non-corrected propagators, respectively.

We performed another MD simulation on the same system using the same calculation conditions except that the time step is increased to 2.0 femtoseconds (this result is shown in Supporting Information). We see that the large oscillations observed in the early stage are even larger and the time to suppress them becomes longer. However, it is found that the time evolution of the kinetic energy of Si atoms is almost the same between these two MD simulations. This result means that time step of 2.0 femtoseconds can be used to do reliable MD simulations on this silicon system. It is encouraging that we can use such a large time step for O(N) FPMD simulations. Here, we

should note that a new efficient method which does not require self-consistent field optimization has been recently proposed[36] within the XL-BOMD framework. Introducing such new techniques to the CONQUEST code may even further accelerate the speed of O(N) FPMD simulations.

3.3.2 Box of 32 water molecules

We take a box of water made up of 32 molecules as our next target. Water is important as a system in its own right, as well as forming the environment for most biological simulations. We performed linear scaling XL-BOMD with ε_L set to 10^{-4}, and using the GGA-PBE functional[37,38] for exchange-correlation, as it describes water better than LDA (we note that the convergence with respect to the grid may be slower for GGA). In Fig. 8 we show the total energy and the ionic and potential energies, T and V_{BO}. We see that there are no initial large oscillations unlike the silicon case, and that T appears to keep increasing during the run. This behavior is seen because we used the micro-canonical ensemble and the simulation time is too short to reach a steady state. Even in such a situation showing fast changes, the averaged fluctuations are ~ 1.1 meV atom^{-1} and good energy conservation is found without any energy drift. These results clearly demonstrate that there are no effects from the grid on the stability and accuracy of MD.

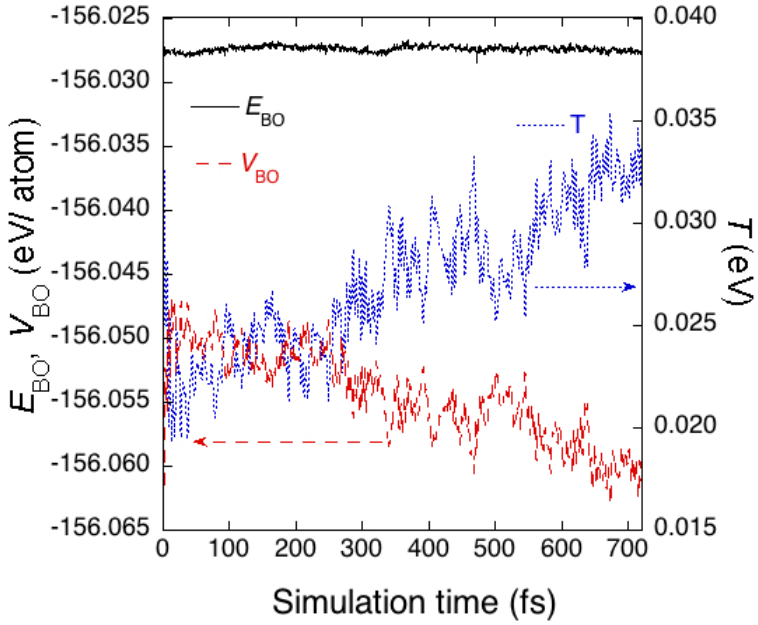

Figure 8: The Born-Oppenheimer total energy profiles of the waterbox system with DZP and PBE: a solid line represents E_{BO}, and red dashed and blue dotted lines characterise its components, V_{BO} and T, respectively (color online).

3.3.3 32,768-atom crystalline silicon

Finally, as a demonstration of the scalability of our approach, we apply our algorithm to a large system: a 32,768 atom crystalline silicon sample. The time evolution of the BO and potential energy are shown in Fig. 9. This is our first substantial attempt to examine the stability of an MD simulation on massive systems. This simulation is conducted under the same conditions as those in the 8-atom system in Fig. 7, except that the time step is set to 2.0 femtoseconds.

We observe some similarities to the previous results. In the early stage of a simulation, large oscillations are seen in the energy, but are gradually suppressed during the MD run. The time to suppress the large oscillations is longer than the one in Fig. 7, but similar to the case using 2.0 femtoseconds for 8-atom crystalline silicon. (See Fig. S1 in the Supporting Information.) Thus, this comes from the difference of the time step, not from the system size. The energy fluctuations after 100 femtoseconds is smaller than 1 meV atom^{-1} and there is no energy drift, as shown in

Fig. 9. Although we only carried out a short MD run, the simulation is expected to remain stable in longer cases without any drift, based on the preceding example of an 8-atom system. Moreover, our approach is expected to ensure great stability on even larger and more complex systems by virtue of high computational efficiency realised in the CONQUEST code.[2,3,39] The average time required for 1 MD step was 1085 seconds using 1024 CPUs (with 16 cores/CPU) of Fujitsu FX10. We are confident that this wall-clock time will be greatly reduced in the near future, because the code is not optimized at present, especially for the part updating X matrices; for simplicity, we now use a simple disk-based I/O procedure to read and write matrix elements of Xs in the previous steps and this part will be improved in the near future.

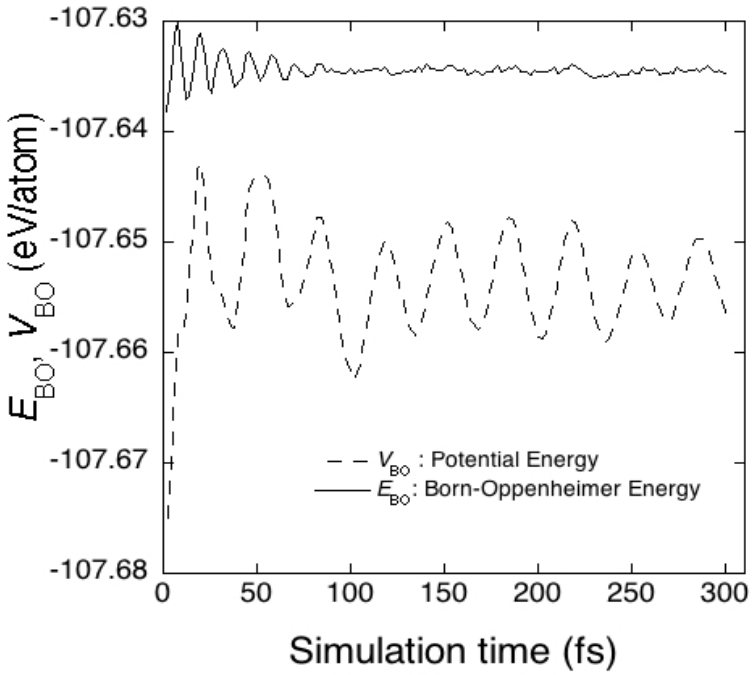

Figure 9: Profiles of the Born-Oppenheimer total energy and potential energy of a 32,768-atom crystalline silicon system with a DZP basis set and LDA functional.

4 Conclusions

In this paper, we have investigated the efficiency, stability and accuracy of MD simulations with the CONQUEST code using the DMM linear scaling approach, to demonstrate large-scale O(N)

FPMD simulations in practice. We first found that accurate MD simulations can be performed by calculating the electronic structure from scratch using the McWeeny procedure at every atomic configuration. This gives excellent energy conservation even with a rather rough tolerance on the convergence of the density matrix minimisation. However, this method requires considerable computational time because it initialises the density matrix at each step, rather than re-utilising it.

Direct re-use of the optimised density matrix reduces computational costs considerably, but causes an unphysical energy drift. In order to achieve both accuracy and efficiency, we have introduced the XL-BOMD formalism, proposed by Niklasson et al., to the CONQUEST code, formulated for non-orthogonal basis functions. The application of XL-BOMD turned out to be much more efficient than the McWeeny approach, especially with the aid of a dissipative force, and good energy conservation was observed. We studied how calculated results depend on two parameters specific to the DMM method: the cutoff range of the L matrix and the tolerance applied to the density matrix minimisation. We found that larger L-ranges resulted in smaller energy fluctuations. Moreover, we found that the MD trajectories from runs with different ranges are almost identical, even when the Born-Oppenhimer total energy was not fully converged. This indicates that, as is well known, the atomic forces converge much faster than the total energy with respect to these two parameters.

As practical applications, we treated crystalline silicon with LDA and liquid water with GGA. For the crystalline silicon, we demonstrated that accurate MD runs can be performed on very large systems, in this case containing 32,768 atoms, but scalable to significantly larger systems. The algorithms presented in this paper are applicable to a canonical ensemble and thus will open doors to more practical calculations on very large and complex systems.

Acknowledgement

The authors thank Lianheng Tong and Takao Otsuka for fruitful discussions. This work is partly supported by KAKENHI projects by MEXT (No. 22104005) and JSPS (No. 26610120 and 26246021), Japan. The support from the Strategic Programs for Innovative Research (SPIRE) and the Computational Materials Science Initiative (CMSI) is also acknowledged. Calculations

were performed using the Numerical Materials Simulator at NIMS, Tsukuba, Japan, K computer at RIKEN Advanced Institute for Computational Science(AICS), Kobe, Japan, and the Fujitsu FX10 system at the Information Technology Center, University of Tokyo, Tokyo, Japan.

Supporting Information Available

We present the comparison of the profiles of Born-Oppenheimer and kinetic energy using different timesteps, 0.5 fs and 2.0 fs and show that the trajectory of the ions are almost the same. The result of crystalline silicon made of 4096 atoms using the initial temperature of 600K is also provided and we see that the energy convergence is excellent.

This material is available free of charge via the Internet at `http://pubs.acs.org/`.

References

(1) Bowler, D. R.; Miyazaki, T. *Rep. Prog. Phys.* **2012**, *75*, 036503.

(2) Bowler, D. R.; Miyazaki, T. *J. Phys.: Condens. Matter* **2010**, *22*, 074207.

(3) Arita, M.; Arapan, S.; Bowler, D. R.; Miyazaki, T. *J. Adv. Simulat. Sci. Eng.* **2014**, in press.

(4) Soler, J. M.; Artacho, E.; Gale, J. D.; García, A.; Junquera, J.; Ordejón, P.; Sánchez-Portal, D. *J. Phys.:Condens. Matter* **2002**, *14*, 2475–2779.

(5) Miyazaki, T.; Bowler, D. R.; Choudhury, R.; Gillan, M. J. *J. Chem. Phys.* **2004**, *121*, 6186–6194.

(6) Hine, N. D. M.; Robinson, M.; Haynes, P. D.; Skylaris, C.-K.; Payne, M. C.; Mostofi, A. A. *Phys. Rev. B* **2011**, *83*, 195102.

(7) Osei-Kuffuor, D.; Fattebert, J.-L. *Phys. Rev. Lett.* **2014**, *112*, 046401.

(8) Bowler, D.; Miyazaki, T.; Truflandier, L. A.; Gillan, M. J. Comment on "Accurate and Scalable O(N) Algorithm for First-Principles Molecular-Dynamics Computations on Large

Parallel Computers". 2014, eprint arXiv:1402.6828, http://arxiv.org/abs/1402.6828 (accessed Sep 22, 2014) .

(9) Car, R.; Parrinello, M. *Phys. Rev. Lett.* **1985**, *55*, 2471–2474.

(10) Payne, M. C.; Teter, M. P.; Allan, D. C.; Arias, T. A.; Joannopoulos, J. D. *Rev. Mod. Phys.* **1992**, *64*, 1045–1097.

(11) Niklasson, A. M. N.; Tymczak, C. J.; Challacombe, M. *Phys. Rev. Lett.* **2006**, *97*, 123001.

(12) Niklasson, A. M. N. *Phys. Rev. Lett.* **2008**, *100*, 123004.

(13) Niklasson, A. M. N.; Steneteg, P.; Bock, N. *J. Chem. Phys.* **2011**, *135*, 164111.

(14) Ohwaki, T.; Otani, M.; Ikeshoji, T.; Ozaki, T. *J. Chem. Phys.* **2012**, *136*, 134101.

(15) Ohwaki, T.; Otani, M.; Ozaki, T. *J. Chem. Phys.* **2014**, *140*, 244105.

(16) Shimojo, F.; Hattori, S.; Kalia, R. K.; Kunaseth, M.; Mou, W.; Nakano, A.; Nomura, K.-i.; Ohmura, S.; Rajak, P.; Shimamura, K.; Vashishta, P. *J. Chem. Phys.* **2014**, *140*, 18A529.

(17) Tsuchida, E. *J. Phys.: Condens. Matter* **2008**, *20*, 294212.

(18) Cawkwell, M. J.; Niklasson, A. M. N. *J. Chem. Phys.* **2012**, *137*, 134105.

(19) Li, X.-P.; Nunes, R. W.; Vanderbilt, D. *Phys. Rev. B* **1993**, *47*, 10891–10894.

(20) Hernández, E.; Gillan, M. J. *Phys. Rev. B* **1995**, *51*, 10157–10160.

(21) Hernández, E.; Gillan, M. J.; Goringe, C. M. *Phys. Rev. B* **1996**, *53*, 7147–7157.

(22) Bowler, D. R.; Miyazaki, T.; Gillan, M. J. *J. Phys.:Condens. Matter* **2002**, *14*, 2781–2798.

(23) Bowler, D. R.; Choudhury, R.; Gillan, M. J.; Miyazaki, T. *Phys. Stat. Sol. (b)* **2006**, *243*, 989–1000.

(24) Hernández, E.; Gillan, M. J.; Goringe, C. M. *Phys. Rev. B* **1997**, *55*, 13485–13493.

(25) Torralba, A. S.; Todorović,; M., V., Brázdová; Choudhury, R.; Miyazaki, T.; Gillan, M. J.; Bowler, D. R. *J. Phys.:Condens. Matter* **2008**, *20*, 294206.

(26) Bowler, D. R.; Gillan, M. J. *Comp. Phys. Commun.* **1999**, *120*, 95–108.

(27) McWeeny, R. *Rev. Mod. Phys.* **1960**, *32*, 335–369.

(28) Palser, A. H. R.; Manolopoulos, D. E. *Phys. Rev. B* **1998**, *58*, 12704–12711.

(29) As each support function is represented by only one PAO, we need not consider the time evolution of S.

(30) Press, W. H.; Flannery, B. P.; Teukolsky, S. A.; Vetterling, W. T. *Numerical Recipes in FORTRAN: The Art of Scientific Computing*, 2nd ed.; Cambridge University Press: Cambridge, UK, 1992.

(31) Niklasson, A. M. N.; Steneteg, P.; Odell, A.; Bock, N.; Challacombe, M.; Tymczak, C. J.; Holmström, E.; Zheng, G.; Weber, V. *J. Chem. Phys.* **2009**, *130*, 214109.

(32) This does not affect the results and larger basis sets are used below.

(33) Perdew, J. P.; Zunger, A. *Phys. Rev. B* **1981**, *23*, 5048–5079.

(34) Verlet, L. *Phys. Rev.* **1967**, *159*, 98–103.

(35) This does not mean the result of MD by using R_L=13bohr is incorrect. The different trajectory may simply come from infinitesimal differences in forces of a chaotic system.

(36) Souvatzis, P.; Niklasson, A. M. N. *The Journal of Chemical Physics* **2014**, *140*, 044117.

(37) Perdew, J. P.; Burke, K.; Ernzerhof, M. *Phys. Rev. Lett.* **1996**, *77*, 3865–3868.

(38) Torralba, A. S.; Bowler, D. R.; Miyazaki, T.; Gillan, M. J. *J. Chem. Theory Comput.* **2009**, *5*, 1499–1505.

(39) Miyazaki, T. Ultra-Large-Scale First-Principles Calculations by the K Computer. NIMS NOW Vol. 11(9), 6, 2013; http://www.nims.go.jp/eng/publicity/nimsnow/2013/vol11_09.html (accessed Sep 22, 2014) .

Graphical TOC Entry

Some journals require a graphical entry for the Table of Contents. This should be laid out “print ready” so that the sizing of the text is correct.
Inside the `tocentry` environment, the font used is Helvetica 8 pt, as required by *Journal of the American Chemical Society*.
The surrounding frame is 9 cm by 3.5 cm, which is the maximum permitted for *Journal of the American Chemical Society* graphical table of content entries. The box will not resize if the content is too big: instead it will overflow the edge of the box.
This box and the associated title will always be printed on a separate page at the end of the document.